AN APPROACH FOR LOCATION OF TRANSMISSION LINE FAULTS BY WAVELET ANALYSIS

Preeti GUPTA **Rabindra N. MAHANTY**
Electrical Engineering Department, National Institute of Technolgy
Jamshedpur, India
erpreetigupta@yahoo.com, rnmahanty2002@yahoo.co.in

Abstract: *A scheme for location of transmission line faults, which uses the wavelet multi resolution analysis approach, is presented. Simulation studies have been carried out on two simulated power system models using EMTP and MATLAB considering wide variations in operating conditions. To illustrate the effectiveness of the proposed approach, the results of the simulation studies are also presented.*

Key Words: *Fault location, wavelet analysis, transmission line.*

1. Introduction

Fault location is an important aspect of transmission line relaying. Accurate location of fault point ensures quick service restoration. By using wavelet analysis, sub-band information can be extracted from the simulated transients, which contain useful fault features. In this paper, it has been shown that the fault features extracted by wavelet analysis of transients can be used for fault location. The approach proposed here involves taking samples of three phase currents at one end of transmission line and carrying out discrete wavelet transform of these samples. A number of fault location techniques have been proposed by different researchers. Some of important ones among them are based on traveling wave [1,2], wavelet analysis [3-10], Artificial Neural Network [11-14] and Fuzzy Logic [15]. Fault location methods based on combined use of neural network, fuzzy logic and wavelet analysis have also been reported [16-18].

An alternative method for fault location based on wavelet analysis is presented in this paper. Extensive simulation studies have been carried out using EMTP and MATLAB considering wide variations in fault location (d), fault inception angle (FIA) and fault resistance (R_F) to illustrate the effectiveness of the proposed approach.

2. Power system models

The single line diagrams of the two power system models which have been considered for the development of the fault location algorithm are shown in Fig. 1 and Fig. 2 respectively [10].

2.1 Model I: Transmission line fed from one end

Line length = 100 km
Source voltage (v_S) = 400 kV
Positive sequence line parameters: R = 2.34 Ω,
L = 95.10 mH, C = 1.24 μF
Zero sequence line parameters: R = 38.85 Ω,
L = 325.08 mH, C = 0.845 μF
Source impedance (Z_S):
Positive sequence impedance =(0.45 + j5) Ω per Phase
Zero sequence impedance = 1.5× Positive sequence impedance
Load impedance (Z_L) = 500-800 Ω per phase with 0.7-0.9 p.f. lagging

2.2 Model II: Transmission line fed from both ends

The parameters of transmission line 1 are same as those considered for transmission line of Model I. The load impedance variations are also same as in case of Model I. The parameters of transmission line 2 and other parameters are as follows:
$R_2 = 1.3\ R_1$, $L_2 = 1.3\ L_1$, $C_2 = C_1$, where suffixes 1 and 2 refer to transmission line 1 and transmission line 2 respectively.
$v_{S2} = 0.95\ v_{S1}$, where $v_{S1}$and v_{S2} are the voltages of source 1 and source 2
δ (Phase difference between v_{S1} and v_{S2}) = 20^0 with v_{S1} leading
Source impedances:
Positive sequence impedance:
Z_{S1} = (0.45 + j5) Ω per phase,
Z_{S2} = (0.34 + j4) Ω per phase.

Zero sequence impedance = 1.5× Positive sequence impedance, for both the sources.

3. Development of the proposed approach

Simulation studies have been carried out for different types of fault under variable operating conditions using EMTP and MATLAB. Wide variations in fault location (*d*), fault resistance (R_F) and fault inception angle (*FIA*) have been considered. Samples of three phase currents have been generated using EMTP, the sampling interval and the data window being 3.3 μs [4] and half cycle respectively. The current samples are taken at one end of transmission line (bus 1) of Fig. 1 & Fig. 2 respectively. Using these current samples wavelet MRA level-1 details [19] have been generated by a MATLAB program that makes use of the 'wavelet toolbox' [20]. The simulation studies carried out for different types of fault for derivation of the fault features are discussed below.

3.1 Wavelet MRA details to be considered

The prerequisite of the proposed approach is that the fault should be detected and also it should be known whether the fault involves ground or not. For detection and classification of transmission line faults, a number of approaches have been proposed by different researchers [10,21-24]. Hence, a priori knowledge of accurate fault detection and classification has been taken for granted. On the basis of extensive simulation studies, it has been found that for different types of faults, wavelet MRA level-1 details, as indicated below, should be considered for the estimation of fault location.

Strategy 1: For all *L-G* and *L-L-G* faults abs (D_{1A}+D_{1B}+ D_{1C}) should be considered. D_{1A}, D_{1B} and D_{1C} are the MRA level-1 details of the three phase currents I_A, I_B and I_C.

Strategy 2: For *A-B* faults *abs* (D_{1A}-D_{1B}), for *B-C* faults *abs* (D_{1B}-D_{1C}), and for *C-A* faults *abs* (D_{1C}-D_{1A}) should be considered.

Strategy 3: For *L-L-L* faults *abs* (D_{1A}-D_{1B}) or *abs* (D_{1B}-D_{1C}) or *abs* (D_{1C}-D_{1A}) should be considered.

Strategy1, Strategy2, Strategy 3 mentioned above have evolved from critical observations based on simulation studies as discussed below.

The sum of MRA level-1 details of the three phase currents *i.e.* D_{1A}+ D_{1B}+ D_{1C} for fault locations at 10% of line length (*d*=0.1) and 80% of line length (*d*=0.8) from bus 1, when $FIA=45^0$ and R_F =5Ω for *A-G* fault in case of Model-I are shown in Fig.3 and Fig.4 respectively. In the figures, time=0 represents the instant of fault inception.

As can be seen from Fig.3 & Fig. 4, the details with significant magnitudes appear later on the time axis after fault inception in case of *d* = 0.8 as compared to the case when *d* = 0.1. The consecutive normalized absolute values, 210 in number, starting from the 16th up to the 225th of the details have been considered for fault location. The normalized absolute values of details are found out by dividing the absolute values of details by the maximum absolute detail value among the 210 detail values. The initial 15 detail values are ignored to avoid the initial oscillations in the detail signature. The consecutive normalized absolute values of detail (starting from the 16th value) till it attains a value of 0.5 or more for the first time for the two above mentioned cases of *A-G* fault for Model-I are shown below:

A-G fault, d = 0.1, FIA = 45^0 and R_F =5Ω
Normalized *abs* (D_{1A}+ D_{1B}+ D_{1C}):
The subsequent values starting from the 1st one are as follows:
0.0000, 0.0003, 0.0009, 0.0003, 0.0002, 0.0293, 0.0203, 0.0113, 0.0186, 0.0192, 0.0145, 0.0131, 0.0297, 0.1133, 0.1142, 0.1154, 0.1560, 0.2055, 0.2419, 0.2721, 0.3112, 0.3264, 0.3413, 0.7592.

A-G fault, d = 0.8, FIA= 45^0 and R_F =5Ω
Normalized *abs* (D_{1A}+ D_{1B}+ D_{1C}):
The initial 112 values are all zeroes. The subsequent values starting from the 113th one are as follows:
0.0063, 0.0073, 0.0022, 0.0043, 0.0611, 0.0643, 0.0854, 0.0715, 0.1219, 0.1143, 0.1571, 0.1422, 0.2101, 0.2412, 0.3487, 0.3621, 0.3507, 0.3318, 0.3269, 0.2940, 0.3521, 1.0000.

From the MRA level-1 detail values shown above, D_{1A}+ D_{1B}+ D_{1C} attains a value of 0.5 or more for the first time in the 24th step (*s* = 24) for *d* = 0.1 and in the 134th step (*s* = 134) for *d* = 0.8 The above relationship between *s* and *d* can be utilized for estimation of fault location. It has been observed that the above relationship between *s* and *d* is the same for all LG and LLG faults considering normalized absolute values as mentioned in strategy 1 i.e. (D_{1A}+ D_{1B}+ D_{1C}). Similar observations have been noticed for Model-II also.

The MRA level-1 details D_{1A} - D_{1B} for fault locations at 10% of line length (d=0.1) and 70% of line length (d=0.7) from bus 1, when FIA=90^0 and R_F =5Ω for *A-B* fault in case of Model-II is shown in Fig. 5 and Fig. 6 respectively.

From Fig. 5 & Fig. 6 it is clear that for *A-B* faults, the normalized absolute value of the detail D_{1A}- D_{1B} attains a value of 0.5 or more for the first time at a later stage for fault at d=0.7 than for fault at d=0.1. This means that, similar to the case of *L-G* faults, a relationship exists between s and d in case of *L-L* faults as well, which is clear from the following observations:

A-B fault, d = 0.1, FIA = 90^0 and R_F =5Ω
Normalised *abs* (D_{1A} - D_{1B}):
The subsequent values starting from the 1st one are as follows:
0.0002, 0.0005, 0.0129, 0.0212, 0.0102, 0.0135, 0.0163, 0.0116, 0.0242, 0.1114, 0.1176, 0.1543, 0.3643, 0.3891, 0.7342.

A-B fault, d = 0.7, FIA= 90^0 and R_F =5Ω
Normalised *abs* (D_{1A} - D_{1B}):
The initial 81 values are all zeroes. The subsequent values starting from the 82nd one are as follows:
0.0024, 0.0034, 0.0056, 0.0072, 0.0043, 0.0065, 0.0076, 0.0068, 0.0054, 0.0601, 0.0624, 0.0709, 0.1198, 0.1154, 0.1143, 0.1481, 0.2156, 0.2354, 0.2482, 0.3451, 0.3662, 0.3543, 0.3376, 0.2804, 0.3334, 0.3609, 1.0000.

D_{1A} - D_{1B} attains a value of 0.5 or more for the first time in 15th step (s = 15) for d = 0.1 and in the 108th step (s = 108) for d = 0.7. The above relationship between s and d can be utilized for estimation of fault location. It has been observed that the relationship between s and d is the same for all LL/LLL faults provided the normalized absolute values of MRA details as mentioned in strategy 2 and strategy 3 are considered. Similar observations have been noticed for Model-I also.

3.2 Effect of variations in *FIA* and R_F

Another important observation is that the proposed fault location approach is applicable for wide variations in *FIA* and R_F. The consecutive normalized absolute values of detail, starting from 16th value till it attains a value of 0.5 or more for two different cases of *A-G* fault occurring at d=0.5 for Model-I and for two different cases of *A-B* fault for Model-II occurring at d=0.7 are shown below.

Model-I: A-G fault, d = 0.5, FIA = 0^0 and R_F =1Ω
Normalised *abs* (D_{1A}+ D_{1B}+ D_{1C}):
The initial 63 values are all zeroes. The subsequent values starting from the 64th one are as follows:
0.0092, 0.0075, 0.0054, 0.0063, 0.0573, 0.0482, 0.0672, 0.0786, 0.0877, 0.0921, 0.1381 0.3085, 0.3334, 0.3292, 0.2960, 0.3101, 0.3261, 0.3391, 0.3491, 0.3541, 0.3012, 0.3390, 0.3687, 1.0000.

Model-I:A-G fault, d = 0.5, FIA = 90^0 and R_F =80Ω
Normalised *abs* (D_{1A}+ D_{1B}+ D_{1C}):
The initial 63 values are all zeroes. The subsequent values starting from the 64th one are as follows:
0.0086, 0.0049, 0.0038, 0.0054, 0.0121, 0.0446, 0.0682, 0.0748, 0.0754, 0.0776, 0.1175, 0.3161, 0.3491, 0.3486, 0.3010, 0.3065, 0.3045, 0.3344, 0.3578, 0.2890, 0.3174, 0.3234, 0.3391, 1.000.

Model-II:A-B fault, d = 0.7, FIA = 0^0 and R_F =1Ω
Normalised *abs* (D_{1A} - D_{1B}):
The initial 80 values are all zeroes. The subsequent values starting from the 81st one are as follows:
0.0380, 0.0525, 0.0617, 0.0624, 0.0651, 0.0683, 0.0876, 0.1001, 0.1276, 0.1601, 0.1819, 0.2156, 0.2652, 0.3373, 0.3501, 0.6563.

Model-II:A-B fault,d= 0.7, FIA = 90^0 and R_F =80Ω
Normalised *abs* (D_{1A} - D_{1B}):
The initial 80 values are all zeroes. The subsequent values starting from the 81st one are as follows:
0.0424, 0.0832, 0.0765, 0.0752, 0.0948, 0.1332, 0.1537, 0.1801, 0.2223, 0.2269, 0.2302, 0.2632, 0.3015, 0.3275, 0.3409, 0.6643.

From the MRA level-1 detail values shown above, it may be observed that, for *A-G* faults at d=0.5 with *FIA* and R_F variable, the normalized value of MRA level-1 detail: D_{1A}+ D_{1B}+ D_{1C} assumes a value of 0.5 or more for the first time in the 87th step (s=87) Similarly, for *A-B* faults at d=0.7 with *FIA* and R_F variable, the MRA level-1 detail D_{1A} - D_{1B} assumes a value of 0.5 or more for the first time in the 96th step (s=96). This shows that the value of s depends on d and remains unaffected by the variations in *FIA* and R_F over a wide range.

Table 1 shows the values of s for fault locations at every 10% of line length (d = 0, 0.1, 0.2, 0.3…..1) in case of *L-G/L-L-G* faults and *L-L/L-L-L* faults for

Model-I & Model-II for variations of 0-100Ω in R_F and 0-90^0 in *FIA*. This table is used as look up table for estimation of fault location.

Table 1
Look up table for different faults in Case of Model-I & Model-II.

Fault location (d)	s			
	Model-I		Model-II	
	LG/LLG	LL/LLL	LG/LLG	LL/LLL
0.0	13	10	8	4
0.1	24	21	19	15
0.2	39	33	33	27
0.3	58	45	52	39
0.4	73	60	67	54
0.5	87	72	81	66
0.6	102	87	96	81
0.7	120	102	114	96
0.8	134	114	130	108
0.9	149	126	145	120
1.0	164	138	160	132

d=Fault location in p.u, s= Step at which the normalized MRA level-1 detail attains a value ≥ 0.5 for the first time.

3.3 The Proposed Algorithm

On the basis of the observations, as detailed above, a fault location algorithm has been developed. The algorithm is given below.

1. Calculate MRA level-1details: D_{1A}, D_{1B} and D_{1C} of the three phase currents.
2. If the fault is *LG/LLG* fault calculate *D*= norm. abs $(D_{1A}+D_{1B}+D_{1C})$, otherwise go to step 3.
3. If the fault is *LL* fault then
   For A-B faults, calculate *D*=norm.abs $(D_{1A}-D_{1B})$;
   For B-C faults, calculate *D*=norm.abs $(D_{1B}-D_{1C})$;
   For C-A faults, calculate *D*=norm.abs $(D_{1C}-D_{1A})$;
   Otherwise go to step 4.
4. If the fault is *LLL* fault then calculate
   D=norm. abs $(D_{1A}-D_{1B})$ or
   D=norm. abs $(D_{1B}-D_{1C})$ or
   D=norm. abs $(D_{1C}-D_{1A})$
5. Find the value of s, the step at which D$\geq$ 0.5 for the first time.
6. Use look up table to estimate fault location.

4. Testing and Results

From Table 1 it is clear that the fault location (*d*) is estimated on the basis of the value of *s* using the technique of Linear Regression which calculates, or predicts, a future value by using existing values. The Linear Regression Technique is explained below:

$$\text{Let} \quad y=a+b.x \tag{1}$$

Where

$b = \{[n\sum xy - (\sum x)(\sum y)]\} / [n\sum x^2 - (\sum x)^2]$

$a = (\sum y - b.\sum x)/n$

n = number of set of known values of x and y.

By using equation (1) the fault location can be estimated for different types of faults under variable operating conditions assuming *s* (step at which the normalized MRA level-1 detail attains a value of 0.5 or more for the first time) as independent variable and *d* (fault location in p.u. of line length) as dependent variable. The predicted value is a y-value for a given x-value. Some representative simulation results are shown in Tables 2,3,4….9.

To illustrate the fault location approach, the case of *A-G* fault for Model-I when $d = 0.36$, $FIA=45^0$ and $R_F = 70\Omega$ may be considered (Table 2). As shown in Table 2, for the above case the value of *s* has been found as 67. Using Linear Regression the unknown value can be predicted from Table 1 using the equation (1).

$a = y - b\,x$

such that $y = \sum y / n$ & $x = \sum x / n$.

From Table 1 it may be observed that

$\sum s = 963$(from col.II, Table I), $\sum d = 5.5$(from col.I, Table I), $\sum sd = 650.8$, $\sum s^2 = 110385$, $(\sum s)^2 = 927369$ & $n = 11$.

Replacing x by *s* & y by *d* where *s* = Step at which the normalized MRA level-1 detail attains a value of 0.5 or more for the first time, *d* = Fault location in p.u. of line length from bus 1 of Fig.1 & Fig 2, using the above data gives

$b = 0.00649188$ & $a = -0.0683317$.

Thus *s* = 67 indicates the estimated fault location d_e (estimated fault location) as:

$d_e = a + b\,s$

$= -0.0683317 + 0.00649188 \times 67$

$= 0.36662$

Therefore, % error in estimation of fault location

$= \{(d_e\text{-}d)/1\}*100\%$

$= \{(0.36662\text{-}0.36)/1\}*100\%$

$= 0.662\%$

Simulation results in case of the 400 kV, 3 phase, 100 km, horizontal formation of conductors transmission line have been presented in Table 2,3… 9 for variations in the values of fault resistance, fault inception angle and fault location for illustrating the validity and accuracy of the proposed method. From the results presented, it can be observed that the maximum error associated with the proposed algorithm is ± 0.759%, which indicates high accuracy.

Table 2
Fault location estimates for A-G Fault in case of Model I

Fault Type	Fault Condition (d,FIA, R_F)	s	d_e	% error
A-G	0.07, 10^0, 80 Ω	21	0.06799	-0.201
	0.15, 0^0, 10 Ω	33	0.14590	-0.410
	0.22, 75^0, 30 Ω	45	0.22380	0.380
	0.36, 45^0, 70 Ω	67	0.36662	0.662
	0.45,90^0, 0 Ω	80	0.45102	0.102
	0.54, 30^0, 0.1 Ω	93	0.53541	-0.459
	0.6, 20^0, 100 Ω	103	0.60033	0.033
	0.77, 60^0, 50 Ω	129	0.76912	-0.088
	0.84, 45^0, 20 Ω	140	0.84053	0.053
	0.90, 10^0, 90 Ω	149	0.89896	-0.104

d_e = Estimated fault location

Table 3
Fault location estimates for B-G fault in case of Model II

Fault Type	Fault Condition (d,FIA, RF)	s	d_e	% error
B-G	0.06, 30^0, 10 Ω	14	0.06076	0.076
	0.17, 60^0, 20 Ω	31	0.17013	0.013
	0.28, 20^0, 1 Ω	48	0.27950	-0.050
	0.38, 0^0, 100 Ω	63	0.37601	-0.399
	0.47, 90^0, 40 Ω	77	0.46608	-0.392
	0.58, 75^0, 30 Ω	94	0.57545	-0.455
	0.65, 45^0, 0.1 Ω	105	0.64622	-0.378
	0.76, 5^0, 20 Ω	123	0.76202	0.202
	0.87, 45^0,70 Ω	140	0.87139	0.139
	0.95, 80^0, 50 Ω	152	0.94860	-0.140

Table 4
Fault location estimates for A-B-G fault in case of Model I

Fault \Type	Fault Condition (d,FIA, R_F)	s	d_e	% error
A-B-G	0.03, 30^0, 10 Ω	16	0.03554	0.554
	0.17, 5^0, 20 Ω	36	0.16537	-0.463
	0.25, 60^0, 90 Ω	50	0.25626	0.626
	0.39, 15^0, 30 Ω	70	0.38610	-0.390
	0.47, 90^0, 05 Ω	83	0.47049	0.049
	0.59, 50^0, 20 Ω	101	0.58735	-0.265
	0.65, 75^0, 1 Ω	111	0.65226	0.226
	0.79, 20^0, 0.1 Ω	132	0.78859	-0.141
	0.88, 45^0, 100 Ω	146	0.87948	-0.052
	0.91, 10^0, 50 Ω	150	0.90545	-0.455

Table 5
Fault location estimates for B-C-G fault in case of Model II

Fault Type	Fault Condition (d,FIA, R_F)	s	d_e	% error
B-C-G	0.04, 10^0, 1 Ω	11	0.04146	0.146
	0.14, 75^0, 10 Ω	26	0.13796	-0.204
	0.27, 0^0, 80 Ω	47	0.27307	0.307
	0.38, 45^0, 30 Ω	64	0.38244	0.244
	0.45, 90^0, 05 Ω	75	0.45321	0.321
	0.55, 30^0, 70 Ω	90	0.54971	-0.029
	0.69, 20^0, 100 Ω	112	0.69125	0.125
	0.76, 60^0, 0.1 Ω	123	0.76202	0.202
	0.89, 45^0, 20 Ω	143	0.89069	0.069
	0.97, 0^0, 50 Ω	155	0.96790	-0.210

Table 6
Fault location estimates for A-B fault in case of Model I

Fault Type	Fault Condition (d,FIA, R_F)	s	d_e	% error
A-B	0.04, 15^0, 10 Ω	14	0.04759	0.759
	0.16, 05^0, 20 Ω	29	0.16173	0.173
	0.25, 30^0, 0.1 Ω	40	0.24543	-0.457
	0.34, 75^0, 100 Ω	52	0.33675	-0.325
	0.49, 45^0, 50 Ω	72	0.48893	-0.107
	0.58, 60^0, 30 Ω	84	0.58024	0.024
	0.66, 75^0, 1 Ω	94	0.65634	-0.366
	0.78, 45^0, 80 Ω	110	0.77809	-0.191
	0.85, 60^0, 40 Ω	119	0.84657	-0.343
	0.91, 90^0, 50 Ω	127	0.90744	-0.256

Table 7
Fault location estimates for B-C fault in case of Model II

Fault Type	Fault Condition (d,FIA, RF)	s	d_e	% error
B-C	0.01, 30^0, 1 Ω	3	0.01479	0.479
	0.12, 15^0, 100 Ω	17	0.11842	-0.158
	0.24, 60^0, 50 Ω	33	0.23687	-0.313
	0.37, 45^0, 30 Ω	51	0.37012	0.012
	0.44, 20^0, 0.1 Ω	60	0.43674	-0.326
	0.58, 75^0, 20 Ω	79	0.57739	-0.261
	0.69, 90^0, 30 Ω	95	0.69583	0.583
	0.77,15^0, 0 Ω	105	0.76986	-0.014
	0.84, 5^0, 80 Ω	115	0.84389	0.389
	0.95, 75^0, 70 Ω	129	0.94753	-0.247

Table 8
Fault location estimates for A-B-C fault in case of Model I

Fault Type	Fault Condition (d,FIA, RF)	s	d_e	% error
L-L-L	0.04, 0^0, 0.1 Ω	14	0.04759	0.759
	0.14, 15^0, 50 Ω	26	0.13890	-0.110
	0.21, 75^0, 30 Ω	35	0.20739	-0.261
	0.37, 35^0, 100 Ω	56	0.36718	-0.282
	0.49, 60^0, 20 Ω	72	0.48893	-0.107
	0.55, 75^0, 40 Ω	80	0.54981	-0.019
	0.67, 20^0, 1 Ω	96	0.67156	0.156
	0.76, 45^0, 10 Ω	108	0.76287	0.287
	0.81, 80^0, 100 Ω	114	0.80852	-0.148
	0.97, 90^0, 80 Ω	135	0.96832	-0.168

Table 9
Fault location estimates for A-B-C fault in case of Model II

Fault Type	Fault Condition (d,FIA, RF)	s	d_e	% error
L-L-L	0.04, 0^0, 0.1 Ω	7	0.04440	0.440
	0.14, 15^0, 50 Ω	20	0.14063	0.063
	0.21, 75^0, 30 Ω	29	0.20726	-0.274
	0.37, 35^0, 100 Ω	51	0.37012	0.012
	0.49, 60^0, 20 Ω	67	0.48856	-0.144
	0.55, 75^0, 40 Ω	75	0.54778	-0.222
	0.67, 20^0, 1 Ω	91	0.66622	-0.378
	0.76, 45^0, 10 Ω	104	0.76246	0.246
	0.81, 80^0, 100 Ω	110	0.80688	-0.312
	0.97, 90^0, 80 Ω	132	0.96973	-0.027

4. Comparison with Existing Scheme

The fault location method proposed here and the method proposed by Chanda et al.[6] are somewhat similar. Both the methods are based on wavelet MRA outputs of three phase currents, which are added/ subtracted depending on the fault type. The variations in the operating conditions considered for the validation of two approaches are also comparable. However, the proposed method has several advantages over the method of Chanda et al.:

(i) Whereas the method proposed by Chanda et al. requires current samples from both ends of line, the proposed method requires current samples from one end of line only.

(ii) The algorithm proposed by Chanda et al. requires the consideration of MRA level-3 output. The proposed algorithm requires the consideration of MRA level-1 output and hence involves lower computational burden in wavelet analysis.

(iii) Apart from computation of MRA details the method proposed by Chanda et al. requires a complicated cubical interpolation technique for estimation of fault location. After computation of MRA details the amount of calculations involved in the proposed approach is much less as compared to that in case of the approach of Chanda et al. as only the step at which the sum/difference of details attains a certain value is needed to be found out.

5. Conclusions

A wavelet analysis based approach for location of transmission line faults has been proposed. The proposed approach uses MRA level-1 details for the purpose of fault location. For *L-G/L-L-G* faults the sum of the details of the three phase currents, for *L-L* faults the difference of the details of the faulty phase currents and for *L-L-L* faults the difference of the details of any two phase currents is to be considered. Location of fault on the basis of MRA level-1 details of the three phase currents ensures less computational burden and fast speed. The greatest advantage of the proposed approach is its simplicity. Results of simulation studies carried out on two typical power system models considering wide variations in fault resistance, fault inception angle and fault location show that the proposed algorithm is capable of accurately locating transmission line faults.

References

1. Zhao W., Song Y. H., Chen W. R., *Improved traveling wave fault locator for power cables by using wavelet analysis*. In: International Journal of Electrical Power and Energy Systems, 23, 2001, p. 403-411.
2. Gilany M., Ibrahim D.K., Eldin E.S.T., *Traveling-Wave-Based Fault-Location Scheme for Multiend-Aged Underground Cable System.* In: IEEE Trans. Power Delivery, 22(1), 2007, p. 82-89.
3. Magnago F.H.,Abur A., *Fault location using wavelets*. In: IEEE Trans. Power Delivery, 13(4), 1998, p. 1475-1480.
4. Abur A.,Magnago F.H., *Use of time delays between modal components in wavelet based fault location*. In: International Journal of Electrical Power and Energy Systems, 22, 2000, p. 397-403.
5. Liang J., Elangovan S., Devotta B.X., *Application of wavelet transform in traveling wave protection.* In: International Journal of Electrical Power and Energy Systems, 22, 2000, p. 537-542.
6. Chanda D., Kishore N.K., Sinha A.K., *A wavelet multi resolution analysis for location of faults on transmission lines.* In: International Journal of Electrical Power and Energy Systems, 25, 2003, p. 59-69.
7. Da Silva M., Oleskovicz M., Coury D.V., *A hybrid fault locator for three-terminal lines based on wavelet transforms.* In: Electric Power Systems Research, 78(11), 2008, p. 1980-1988.
8. Yusuff A., Fei C., Jimoh A.A., Munda J.L., *Fault location in a series compensated transmission line based on wavelet packet decomposition and support vector regression*. In: Electric Power Systems Research , 8(7), 2011, 1258-1265.
9. Jung C.K., Lee J.B., Wang X.H., Song Y.H, *Wavelet based noise cancellation technique for fault location on underground power cables*. In: Electric Power Systems Research, 77(10), 2007, p. 1349-1362.
10. Mahanty R. N., Gupta Dutta P. B, *An Improved Method for digital Relaying of Transmission Lines*. In: Electric Power Components and Systems, 32(10), 2004, p. 1013-1030.
11. Thukaram D., Khincha H. P., Vijaynarasimha H. P., *Artificial Neural Network and Support Vector Machine Approach for Locating Faults in Radial Distribution System.* In: IEEE Trans. Power Delivery, 20(2), 2005, p. 710-721.
12. Osman A.H., Abdelazim T., Malik O. P., *Transmission Line Distance Relaying Using On-Line Trained Neural Networks.* In: IEEE Trans. Power Delivery, 20(2), 2005, p. 1257-1264.
13. Gracia J., Mazón A. J., & Zamora I.R.Y., *Best ANN Structures for Fault Location in Single and Double-Circuit Transmission Lines.* In: IEEE Trans. Power Delivery, 20(4), 2005, p. 2389-2395.
14. Joorabian M., Taleghani S.M.A.A, Aggarwal R.K., *Accurate fault locator for EHV transmission lines based on radial basis function neural networks*. In: Electric Power Systems Research, 71(3), 2004, p. 195-202.
15. Sadeh J., Afradi H., *A new and accurate fault location algorithm for combined transmission lines using Adaptive Network-Based Fuzzy Inference System.* In: Electric Power Systems Research, 79(11), 2009, p. 1538-1545.
16. Chunju F., Lai K.K., Chan W.L., Weiyong Y. *et. al., Application of wavelet fuzzy neural network in locating single line to ground fault (SLG) in distribution lines*. In: Electrical Power and Energy System, 29(6), 2007, p. 497-503.
17. Jung C.K., Lim K.H., Lee J.B., Klockl B., *Wavelet and neuro-fuzzy based fault location for combined transmission systems.* In: Electrical Power and Energy System, 29, 2007, p. 445-454.
18. Jayabharata M.R., Mohanta D.K., *A wavelet-fuzzy combined approach for location and classification of transmission line faults.* In: International Journal of Electrical Power & Energy Systems, 29(9), 2007, p. 669-678.
19. Mallet S.G., *A theory for multiresolution signal decomposition: the wavelet representation*. In: IEEE Trans. Pattern Analysis and Machine Intelligence, 11[7], 1995, P. 674-693.
20. Misiti M., Misiti Y., Openheim G., Poggi J., *Wavelet toolbox for use with Matlab*. The Mathworks, Natick, MA, 1996.
21. Osman A. H., *Transmission Line Distance Protection Based on Wavelet Transform.* In: IEEE Trans. Power Delivery , 19(2), 2004, p. 515-523.
22. He Z., Fu L., Lin S., Bo Z.**,** *Fault Detection and Classification in EHV Transmission Line Based on Wavelet Singular Entropy*. In: IEEE Trans. Power Delivery, 25(4), 2010, p. 2156-2163.
23. Liang J.,Elangovan S., Devotta J.B.X., *A wavelet multiresolution analysis approach to fault detection and classification in transmission lines*. In: Electrical Power and Energy Systems, 20(5}, 1998, p. 327-332.
24. Zhao W., Song Y.H., Min Y., *Wavelet analysis based scheme for fault detection and classification in underground power cable systems*. In: Electric Power Systems Research, 53, 2000, p. 23-30.

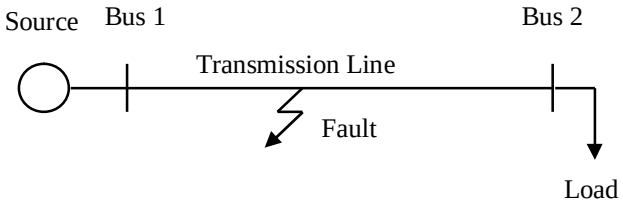

Fig. 1. Model I: A faulted transmission line fed from one end.

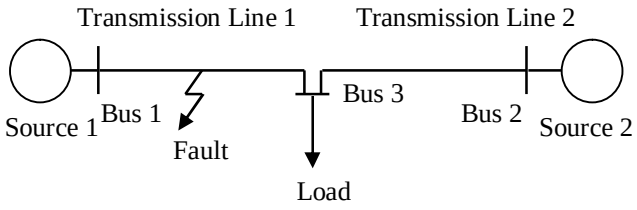

Fig.2. Model II: A faulted transmission line fed from both ends.

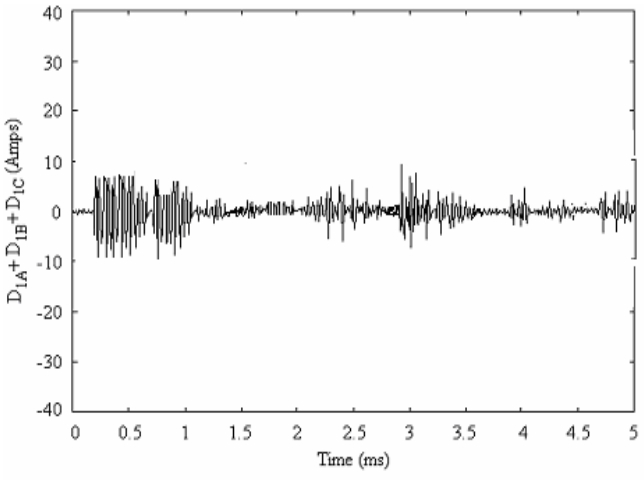

Fig. 3. $D_{1A} + D_{1B} + D_{1C}$ in case of *A-G* fault for Model-I when d=0.8, FIA=45^0 and R_F =5Ω.

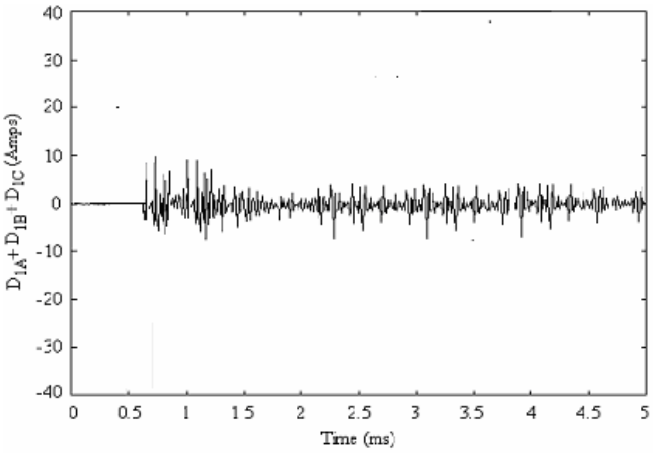

Fig. 4. . $D_{1A} + D_{1B} + D_{1C}$ in case of *A-G* fault for Model-I when d=0.8, FIA=45^0 and R_F =5Ω .

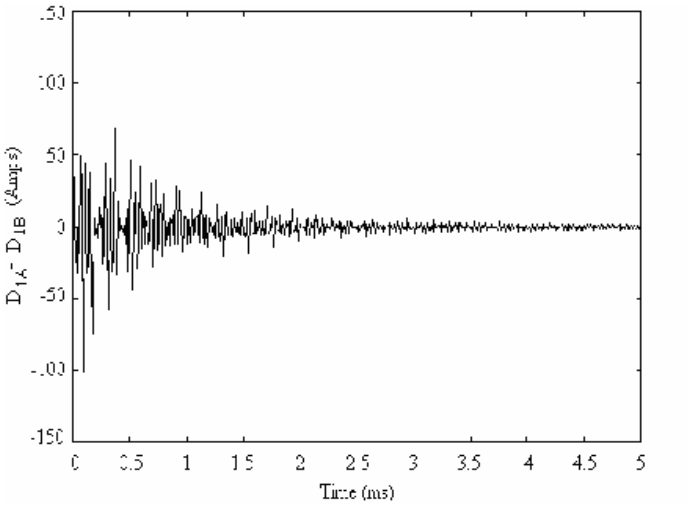

Fig. 5. D_{1A}-D_{1B} in case of *A-B* fault for Model-II when d=0.1, FIA=90^0 and R_F =5Ω.

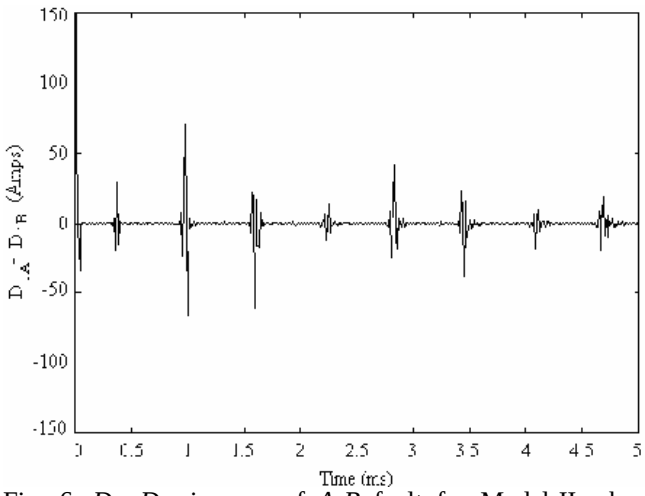

Fig. 6. D_{1A}-D_{1B} in case of *A-B* fault for Model-II when d=0.7, FIA=90^0 and R_F =5Ω.